BMC Cancer

RESEARCH Open Access

Early prediction of liver metastasis in pancreatic cancer using routine clinical data: an externally validated machine learning model

Yeo Gyeong Ko[1], See Young Lee[2,3], Won Kyu Lee[2,3], Ji Hoon Park[4], Sang Hoon Lee[5], Kyung In Shin[6], Jiyoung Keum[7], Jee Hoon Kim[1,2], Jung Hyun Jo[2,3], Sung Ill Jang[2,3], Jae Hee Cho[2,3], Galam Leem[1,2], Moon Jae Chung[1,2], Jeong Youp Park[1,2], Seungmin Bang[1,2], Seung Woo Park[1,2], Seung Up Kim[1,2,8,9] and Hee Seung Lee[1,2*]

Abstract

Background Liver metastasis at the time of pancreatic cancer diagnosis plays a critical role in treatment planning owing to its strong association with poor prognosis. However, they often remain undetected because of the limited sensitivity of conventional imaging and biomarkers. Previous studies have primarily focused on postoperative liver metastasis or relied on complex nonroutine variables (e.g., liquid biopsy and radiomics), which limit scalability and real-world applicability. To address this unmet need, we applied an machine learning (ML) approach chosen for its interpretability, developing a simple, real-time prediction model that uses only routine clinical data available at diagnosis.

Methods We retrospectively enrolled 2,657 patients with pancreatic cancer from a tertiary centre to develop the Liver Metastasis in Pancreatic Cancer (LiMPC) model. The model was trained using 21 routinely available clinical variables and compared across four ML algorithms. The best performing model (extreme gradient boosting) was calibrated using isotonic regression and externally validated in five independent hospitals ($n=272$). Model performance was evaluated using AUROC, sensitivity, specificity, negative predictive value, positive predictive value, and calibration plots. Clinical utility was assessed with decision curve analysis, and feature contributions were interpreted using SHapley Additive exPlanations (SHAP).

Results The fine-tuned LiMPC model achieved strong external validation performance (AUROC = 0.78, sensitivity = 0.81, specificity = 0.55) with robust calibration and consistent clinical net benefit. SHAP interpretation identified CA19-9, CEA, GGT, and age as key predictors, consistent with established biomarkers of advanced disease. In the subgroup analysis, the model achieved particularly strong discrimination in older (AUROC = 0.82) and male (AUROC = 0.82) patients, suggesting demographic influences on metastatic risk. In supplementary analyses, baseline

*Correspondence:
Hee Seung Lee
lhs6865@yuhs.ac

Full list of author information is available at the end of the article

predictors remained consistent among patients who later developed liver metastasis, reinforcing the model's biological plausibility and clinical relevance.

Conclusions LiMPC is an externally validated, interpretable tool for liver metastasis risk stratification using routinely collected clinical data. As a hypothesis-generating tool, it demonstrates how simple clinical variables can provide decision support when imaging results are inconclusive, offering a practical framework for future prospective validation and clinical implementation.

Keywords Pancreatic cancer, Liver metastasis, Machine learning, Clinical decision support

Background

Pancreatic cancer continues to have a poor prognosis, with less than 10% of patients surviving beyond five years [1, 2]. Globally, its incidence increased by approximately 144.6% between 1990 and 2021 [1]. Approximately 80% of patients have distant metastases at diagnosis, with the liver being the most common metastatic site (37%–50%) [3–6]. Although the early detection of liver metastases in pancreatic cancer is crucial for improving patient outcomes [7], accurate identification at initial diagnosis remains challenging, with radiologically occult metastases frequently missed (6.0%–9.7%) [8, 9]. Even advanced imaging modalities demonstrate suboptimal sensitivity, with magnetic resonance imaging (MRI) detecting only 60–91% and computed tomography (CT) around 50% of subcentimetre (< 1 cm) liver metastases [10–12]. These diagnostic limitations frequently lead to unnecessary surgeries, delayed systemic chemotherapy, and inaccurate prognostic assessment [13].

Historically, major advances in cancer therapy were driven by progress in early detection and improved biological understanding [14]. The evolution of precision oncology began with the discovery that tamoxifen efficacy depended on hormone receptor status [15] and progressed with therapies targeting HER2 and BCR-ABL, establishing the principle that biomarker-driven patient selection is essential for optimized outcomes [14, 16]. Today, the expanding use of circulating tumor-derived DNA (ctDNA) and sophisticated imaging enables earlier, more personalized therapeutic strategies—yet these advances underscore the persistent need for robust, clinically practical biomarkers [17].

Despite major advancements in biomarker research, early detection of pancreatic cancer remains challenging, and predicting liver metastasis at initial diagnosis is equally difficult. Among existing markers, carbohydrate antigen 19-9 (CA19-9) has historically been the most widely used biomarker for diagnosis, prognosis, and disease monitoring. However, its diagnostic performance is limited by poor specificity across benign and malignant conditions and by its unreliability in Lewis antigen-negative patients [18, 19]. More recently, novel candidates such as serum exosomal hsa-let-7f-50 and SATB2 have been proposed, offering insights into the biological mechanisms of metastasis and the tumor immune microenvironment [20, 21]. Nevertheless, these approaches are constrained by small cohorts, high costs, and the need for specialized molecular platforms, which limit their scalability in daily clinical practice. In routine practice, pancreatic cancer metastasis is still assessed primarily by CT or MRI, which often miss small or early lesions.

In this context of persistent diagnostic challenges and practical limitations of current biomarker strategies, we developed an machine learning (ML) model—Liver Metastasis in Pancreatic Cancer (LiMPC), to predict liver metastasis at the time of pancreatic cancer diagnosis, using routinely available clinical variables. By leveraging accessible data from electronic medical records, LiMPC offers a cost-effective, interpretable, and generalizable solution to complement conventional imaging and enable early risk stratification in real-world settings.

Methods

We followed the Transparent Reporting of a Multivariable Prediction Model for Individual Prognosis or Diagnosis (TRIPOD) checklist for reporting (Additional file 2) [22].

Study population

We retrospectively analysed 2,657 patients with pancreatic cancer as the derivation cohort: "No liver metastasis at diagnosis (No meta)" group (N = 1,976) and "Liver metastasis at diagnosis (Meta)" group (N = 681), using data from the Severance Hospital in South Korea (Fig. 1, Additional file 1: Supplementary Table S1). All participants were adult patients aged ≥ 19 years who were first diagnosed between 2006 and 2021 at the Severance Hospital. The data collection was completed in 2021.

For external validation, data were collected from five additional hospitals: Ewha Womans University Seoul Hospital, Konkuk University Medical Center, Keimyung University Dongsan Hospital, Gangnam Severance Hospital, and Yongin Severance Hospital, totalling 272 patients. In the external validation group, 190 patients were categorised as "No meta," whereas 82 patients were categorised as "Meta". All were adult patients aged ≥ 19 years who were first diagnosed with pancreatic cancer between 1 January 2008 and 31 December 2024. For both

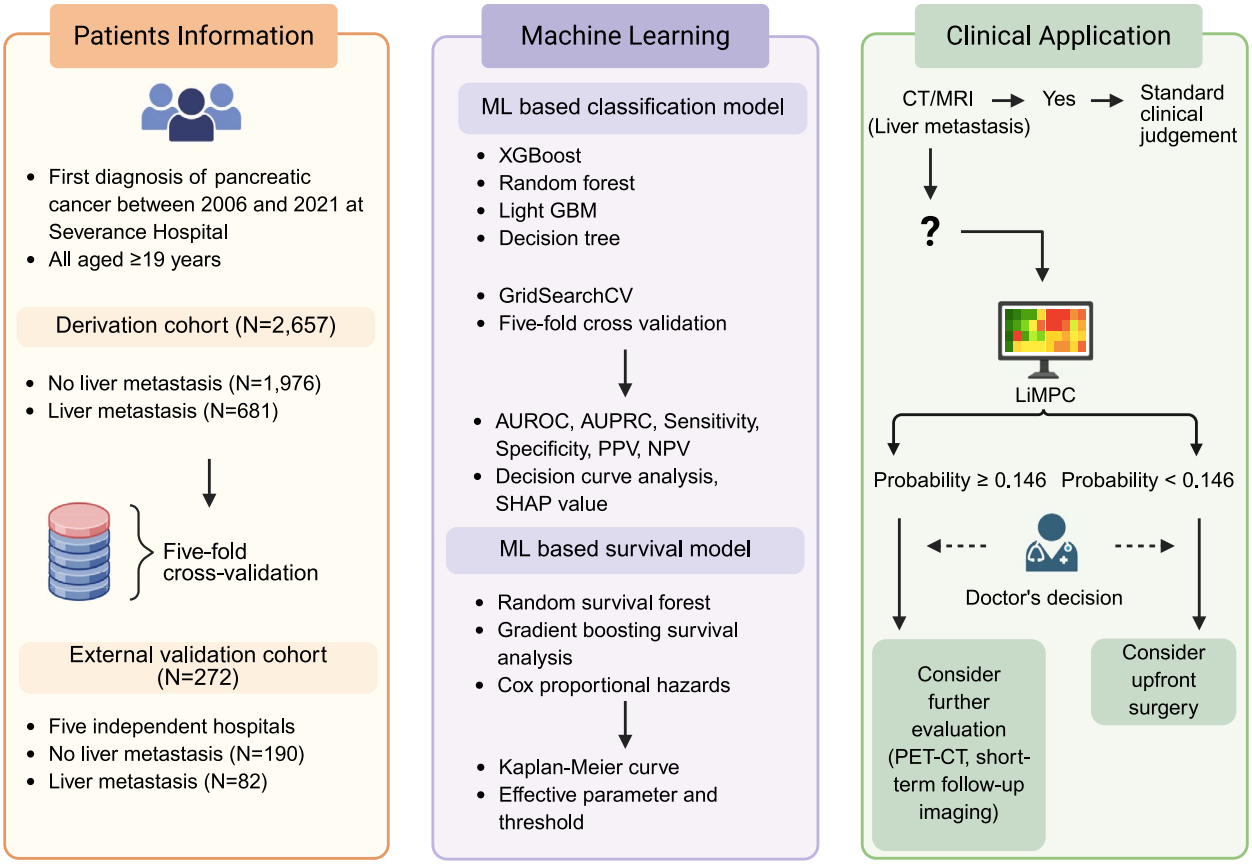

Fig. 1 Overview of patient information, model structure, and clinical implications. Patients newly diagnosed with pancreatic cancer from 2006 to 2021 were included, comprising a derivation cohort ($n=2,657$) and an external validation cohort ($n=272$). Four machine learning models were compared using area under the receiver operating characteristic curve, positive predictive value, and negative predictive value and three survival models were used to identify prognostic thresholds. The Clinical Application panel illustrates how the web-based Liver Metastasis in Pancreatic Cancer (LiMPC) calculator can support real-world decision-making using routine input values. For instance, a 65-year-old male patient with routine lab results (e.g., CA19-9: 25, CEA: 2.4, albumin: 3.9) yields a predicted risk of 14.75%, exceeding the high-risk threshold (≥ 0.146) and prompting further evaluation. Top contributing features are visualized using SHapley Additive exPlanations (SHAP) to enhance interpretability. Created with BioRender.com

derivation and external validation cohorts, follow-up was completed at the observation period or upon patient death, loss to follow-up, or diagnosis of liver metastasis.

Data collection and outcome

Data were collected from the electronic medical records and de-identified. We used ICD-10 codes to identify patients and extracted 21 parameters available at the time of diagnosis, including patient information (age, sex, and body mass index [BMI]), medical history (diabetes mellitus [DM] and hypertension [HTN]), laboratory results (haemoglobin [Hb], platelets [PLT], blood urea nitrogen [BUN], creatinine [Cr], Na, potassium [K], aspartate aminotransferase [AST], alanine aminotransferase [ALT], total bilirubin, albumin [Alb], international normalized ratio [INR], gamma-glutamyl transferase [GGT], total cholesterol, and alkaline phosphatase [ALP]), and biomarkers (carcinoembryonic antigen [CEA] and CA19-9).

Liver metastasis at diagnosis was defined as the metastasis detected on baseline staging CT or MRI, or reported within 30 days of diagnosis to account for subtle lesions that may appear shortly after initial imaging in routine clinical workflows.

Model strategy

ML-based prediction and interpretation of liver metastasis at diagnosis

To predict liver metastasis at diagnosis, we applied tree-based ML algorithms, including the decision tree (DT), random forest (RF), Light Gradient Boost Machine (LightGBM), and Extreme Gradient Boosting (XGBoost) [23]. We performed five-fold cross-validation on the derivation cohort by splitting it into five subsets. In each iteration, four subsets were used for training, and the remaining one served as the internal validation. Out-of-fold (OOF) predictions from all folds were aggregated to calculate the area under the receiver operating characteristic curve (AUROC) and area under the precision-recall curve (AUPRC), minimizing data bias, enhancing generalisability, and allowing fair model comparison.

Model discrimination was further assessed by calculating AUROC and AUPRC in an independent external validation cohort.

The best-performing models were further tuned using grid search within a five-fold cross-validation framework to optimize hyperparameters and prevent overfitting. A fixed risk threshold derived from cross-validation was applied unchanged to the external cohort to prevent data leakage. Predicted probabilities were then calibrated in the derivation cohort using isotonic regression, and calibration was assessed in the external validation cohort using calibration plots. Finally, to evaluate clinical utility, decision curve analysis (DCA) was performed, to calculate the net benefit by balancing true positives against false positives across a range of threshold probabilities, comparing the model with default strategies such as treating all or treating none [24]. For model interpretability, SHapley Additive exPlanations (SHAP) analysis was conducted to quantify each feature's contribution to the prediction [25]. Heatmaps of SHAP effects and interaction values were generated, focusing on the three feature pairs with the strongest interactions to explore their influence on clinical decision thresholds.

To assess generalisability and clinical relevance, subgroup analyses were performed based on age and sex. An age cutoff of 60 years was applied, based on prior studies reporting that pancreatic cancer risk factors and associated biological and clinical characteristics differ before and after age 60 [26]. We hypothesized that a similar distinction might also exist in the development of liver metastasis.

As a supplementary analysis, we further examined whether key variables identified by the ML classification models in the initially "No meta" group were associated with subsequent metastatic events. ML-based survival analyses using Cox proportional hazards (CPH), random survival forest (RSF), and gradient boosting survival analysis (GBSA) were applied. This approach validated that baseline predictors of metastatic risk were consistently linked to long-term outcomes, thereby reinforcing the clinical validity of the model. Model performance was assessed with concordance index and Brier score, and key variables from RSF were further interpreted using SHAP. Kaplan–Meier survival curves were generated to visualize risk stratification with optimal thresholds defined as the cut-points yielding the lowest log-rank test P values while ensuring at least 50 patients per group.

Development of web-based risk calculator

To enhance clinical usability, we developed a publicly accessible, web-based calculator that implements the final LiMPC model and provides SHAP-based feature interpretation for each prediction. The tool is intended to support decision-making in routine clinical settings and is available at: https://choiko9120-8tfgwrh3mrcypkwp2ep8s9.streamlit.app/. The application was developed using Streamlit (https://streamlit.io/), an open-source Python framework for building interactive data-driven applications.

Statistical analysis

Data are expressed as medians with the first and third quartiles and n (%) (Additional file 1: Supplementary Table S1). Missing data were handled by replacing them with the median values of the derivation cohort (Additional file 1: Supplementary Table S2). Diagnostic accuracy was evaluated in terms of sensitivity, specificity, positive predictive value (PPV), and negative predictive value (NPV), AUROC, AUPRC. 95% confidence intervals (CIs) were calculated for AUROC and AUPRC. All ML and statistical analyses were conducted using Python (version 3.12.7), and statistical significance was set at $P < 0.05$.

Results

A total of 2,657 patients were included in the derivation cohort, comprising 1,976 patients in the "No meta" group and 681 in the "Meta" group. The external validation cohort consisted of 272 patients, comprising 190 in the "No meta" group and 82 in the "Meta" group. The baseline patient characteristics are summarised in Additional file 1: Supplementary Table S1. The median age was 66.0 (58.0, 73.0) years in the derivation cohort and 67.0 (59.0, 74.0) years in the external validation cohort ($P = 0.191$). Regarding the cancer biomarkers CEA and CA19-9, no significant differences were observed between the groups. For CA19-9, the derivation group had a median value of 268.0 (35.0, 1720.0), whereas the external validation group had a median value of 159.0 (28.3, 1370.0). For CEA, the median value in the derivation group was 4.1 (2.2, 11.4) compared to 3.6 (2.1, 10.2) in the external validation group.

We compared four ML algorithms (XGBoost, RF, LightGBM, and DT) to predict liver metastasis at diagnosis. In the derivation cohort, based on OOF predictions, XGBoost, RF and LightGBM achieved similar AUROC values of 0.75, followed by DT with 0.70 (Additional file 1: Supplementary Table S3). Given the diagnostic purpose of the model, we prioritised the sensitivity, predefined at ≥ 0.85. After isotonic calibration, a threshold probability of 0.146 was selected to achieve the target sensitivity. Model performance across derivation and external cohorts at fixed sensitivity cutoffs is summarised in Additional file 1: Supplementary Table S3. In the derivation cohort, fine-tuned XGBoost demonstrated the most balanced performance, with a sensitivity of 0.85, specificity of 0.45, PPV of 0.35, and NPV of 0.90. Although RF achieved the same AUROC, its specificity was lower.

Based on these results, XGBoost was selected as the final model for subsequent analyses. In the external validation cohort, fine-tuned XGBoost achieved an AUROC of 0.78 (95% CI: 0.72–0.83), with a sensitivity of 0.81, specificity of 0.55, PPV of 0.43, and NPV of 0.87 (Fig. 2, Additional file 1: Supplementary Table S3). As shown in Fig. 3A, the calibration curve indicated good agreement between predicted and observed risks. The DCA curve (Fig. 3B) further highlighted the clear clinical benefits of LiMPC across threshold probabilities ranging from 1 to 63%.

In the SHAP analysis, CA19-9, CEA, GGT, and age levels showed the highest impact on predicting liver metastasis (Fig. 4A, 4B). Higher CA19-9 and CEA levels were associated with an increased predicted risk whereas older age demonstrated a protective effect. In the SHAP heatmap (Fig. 4C), the strongest interaction was observed between CA19-9 and CEA (0.065), followed by Na and CA19-9 (0.029), and age and GGT (0.019). When CA19-9 exceeded 1,144 U/mL and CEA exceeded 7.95 ng/mL, the predicted probability markedly shifted toward liver metastasis, and lower Na levels (< 138 mmol/L) similarly increased the predicted risk (Additional file 3: Supplementary Fig. S1). In contrast, age > 70 years was associated with a reduced likelihood of metastasis (Fig. 4A, Additional file 4: Supplementary Fig. S2).

In the subgroup analysis, among patients aged ≥ 60 ($n = 199$), the model achieved an AUROC of 0.82, sensitivity of 0.84, and specificity of 0.57. In contrast, among those aged < 60 years ($n = 73$), performance was lower (AUROC = 0.67, sensitivity = 0.71, specificity = 0.48). For sex-based subgroups, the model achieved an AUROC of 0.82, sensitivity of 0.85, and specificity of 0.48 in males ($n = 137$), and an AUROC of 0.76, sensitivity of 0.74, and specificity of 0.61 in females ($n = 135$). These results indicate that the model performs better in older patients and in males (Table 1).

As part of the supplementary survival analysis, RSF (C-index = 0.602, Brier score = 0.202), CPH (C-index = 0.615, Brier score = 0.165), and GBS (C-index = 0.602, Brier score = 0.202) were evaluated, with RSF showing the highest overall performance. Within the RSF model of the "No meta" group, we identified the top four predictive variables and their optimal thresholds. The thresholds, determined via log-rank testing with a minimum of 50 patients per group, were: CEA > 130.0 ng/mL ($P < 0.001$), GGT > 82.0 IU/L ($P < 0.001$),

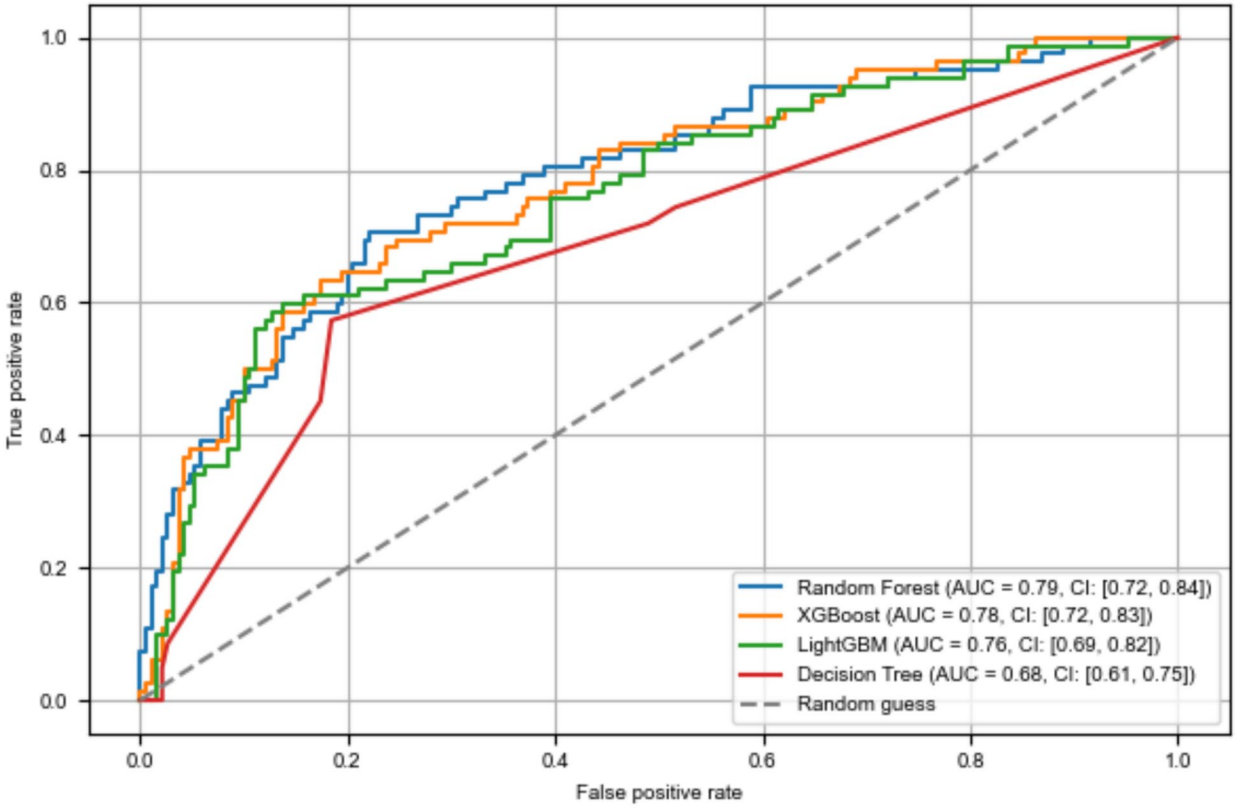

Fig. 2 AUROC of external validation cohort across four models. The performance of four models was evaluated using external datasets from five independent hospitals. Random forest demonstrated the highest area under the receiver operating characteristic curve (AUROC), at 0.79 (95% CI: 0.72–0.84), followed by extreme gradient boosting (XGBoost), at 0.78 (95% CI: 0.72–0.83)

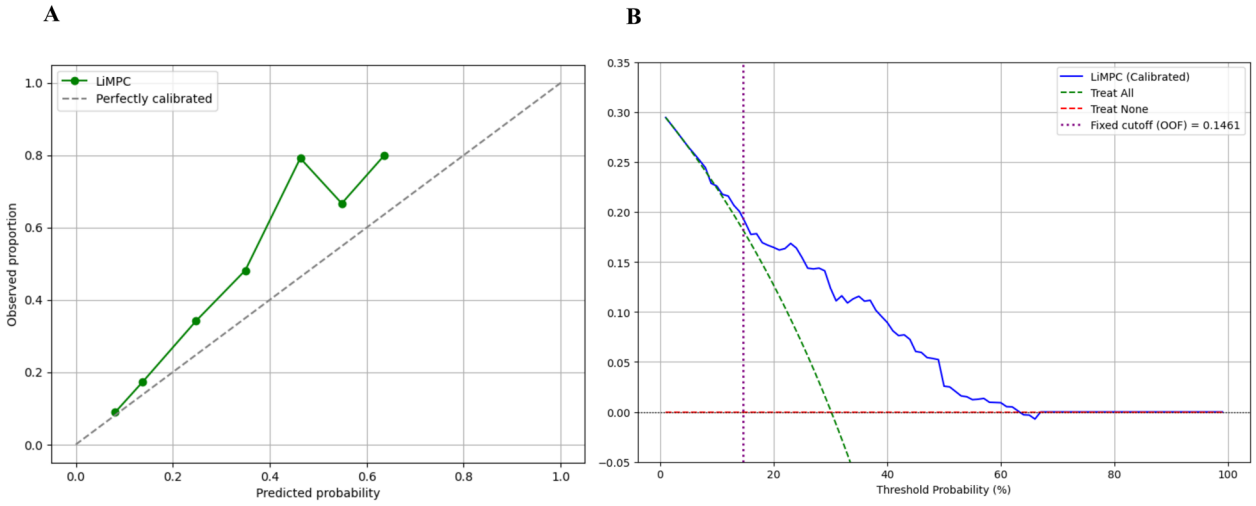

Fig. 3 Calibration and decision curve analysis of the LiMPC model. **A** Calibration plot of the Liver Metastasis in Pancreatic Cancer (LiMPC) model after isotonic regression in the external validation cohort. The green line represents the agreement between predicted probabilities and observed outcomes. The dashed diagonal line indicates perfect calibration. The LiMPC model demonstrated good agreement between predicted and actual risk across the probability spectrum. **B** Decision curve of the LiMPC model (blue line). The blue line exceeds both the "treat-all" (green dashed line) and "treat-none" (red dashed line) strategies across a threshold probability range up to 63%, indicating improved clinical decision-making across a wide spectrum of risk tolerance. The vertical dotted line represents the selected cutoff probability of 0.146, which was chosen to prioritize sensitivity (≥ 85%) in clinical triage

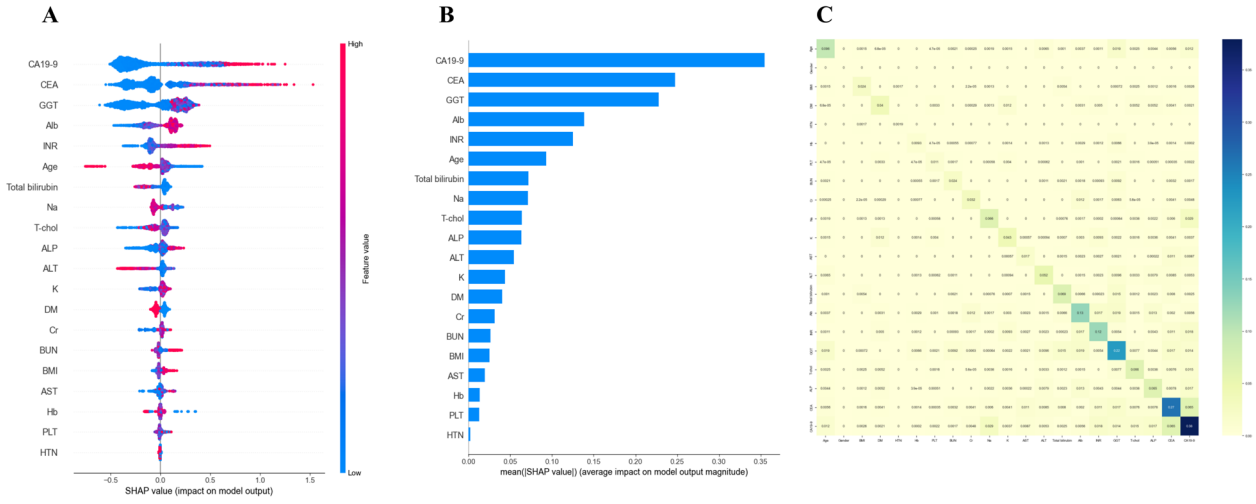

Fig. 4 SHAP analysis for external validation using the fine-tuned XGBoost model. Fine-tuned Extreme Gradient Boosting (XGBoost) was used for SHapley Additive exPlanations (SHAP) evaluation. In plots (**A**) (Beeswarm summary plot) and (**B**) (bar plot), carbohydrate antigen 19-9 (CA19-9), carcinoembryonic antigen (CEA), gamma-glutamyl transferase (GGT), and age showed the key predictive contributions. Plot (**C**), a SHAP interaction heatmap, illustrates pairwise interactions between features, where cooler transitions from deep blue to yellow indicate strong to weak interactions, respectively

Table 1 Model performance in demographic subgroups

	AUROC	AUPRC	Sensitivity	Specificity
Old patients (≥ 60 years, $n = 199$)	0.82 (0.76–0.88)	0.67 (0.55–0.80)	0.84	0.57
Young patients (< 60 years, $n = 73$)	0.67 (0.52–0.80)	0.48 (0.31–0.71)	0.71	0.48
Male ($n = 137$)	0.82 (0.74–0.89)	0.72 (0.60–0.86)	0.85	0.48
Female ($n = 135$)	0.76 (0.66–0.84)	0.54 (0.38–0.71)	0.74	0.61

CA19-9 > 16,600.0 U/mL ($P < 0.001$), and age > 73 years ($P < 0.001$) (Fig. 5A–5E). For each variable, the selected threshold significantly stratified patients in terms of time to metastasis, based on the log-rank test ($P < 0.05$). In the surgical subgroup within the "No meta" cohort ($n = 263$), GGT, age, platelet count, and total bilirubin were identified as relevant predictors (Fig. 6A). The corresponding thresholds were: GGT > 68.0 IU/L ($P = 0.001$), total bilirubin > 2.5 mg/dL ($P = 0.002$), CEA > 5.0 ng/mL ($P = 0.992$), and CA19-9 > 50.0 U/mL ($P = 0.069$) (Fig. 6B–6E).

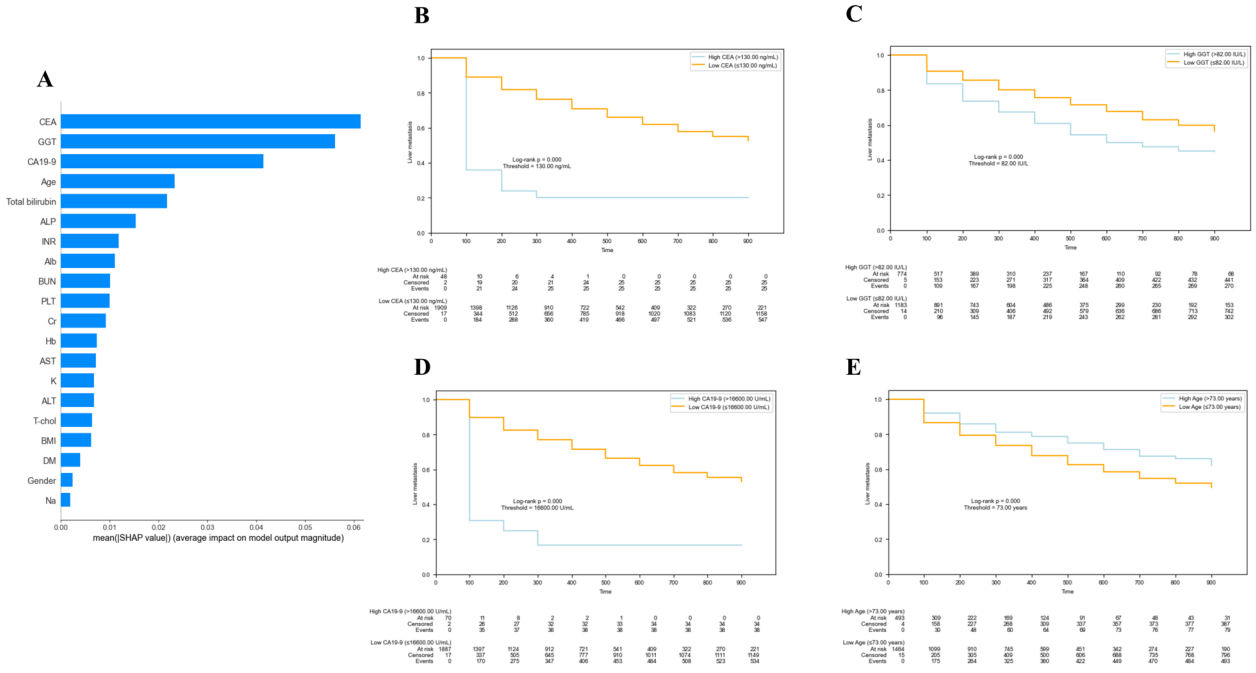

Fig. 5 SHAP analysis and Kaplan–Meier curves for key clinical predictors. **A** SHapley Additive exPlanations (SHAP) analysis using the random survival forest model. Carcinoembryonic antigen (CEA), gamma-glutamyl transferase (GGT), carbohydrate antigen 19–9 (CA19-9), and age were identified as the most important predictive features. Subsequently, clinically relevant features were selected. For each selected feature, a log-rank test was performed to divide patients into two groups using the optimal threshold, which minimized the log-rank *P* value while ensuring that each group included at least 50 patients. **B** Kaplan–Meier survival curves stratified by CEA levels using a threshold of 130.0 ng/mL ($P < 0.001$). **C** Kaplan–Meier survival curves stratified by GGT levels using a threshold of 82.0 IU/L ($P < 0.001$). **D** Kaplan–Meier survival curves stratified by CA 19–9 levels using a threshold of 16,600.0 U/mL ($P < 0.001$). **E** Kaplan–Meier survival curves stratified by age with a threshold of 73 years ($P < 0.001$)

Discussion

In the present study, we developed and externally validated an ML-based tool, termed LiMPC, to predict liver metastasis in patients with pancreatic cancer, using only routine clinical and laboratory variables. Our model achieved robust external performance (AUROC of 0.78, a sensitivity of 0.81, a specificity of 0.55, and an NPV of 0.87) and may serve as a complementary diagnostic aid in clinical practice.

Although prior studies have investigated liver metastasis in pancreatic cancer, most have focused on postoperative recurrence rather than metastasis present at the time of diagnosis. As summarised in Additional file 1: Supplementary Table S4, many of these studies rely on complex inputs such as histopathologic data, transcriptomics, or liquid biopsy biomarkers, which require specialized infrastructure and incur high costs, thereby limiting their real-world clinical applicability [27–29]. In contrast, LiMPC was specifically developed to address these limitations, focusing on scalability, accessibility, and ease of integration, making it well suited for early stratification or use in resource-constrained settings. To the best of our knowledge, LiMPC is the first externally validated model for this purpose.

SHAP analysis highlighted CEA, CA19-9, GGT and age as important contributors. Among these, CEA and CA19-9 were the most influential predictors, consistent with previous studies linking elevated levels of these markers to advanced pancreatic cancer [30–34]. Unlike prior studies that defined cutoffs based solely on statistical associations (e.g., CEA > 7.0 ng/mL and CA19-9 > 305 U/mL) [35], our ML-based thresholds (CEA > 7.95 ng/mL and CA19-9 > 1,144 U/mL) represent data-driven decision boundaries shaped by nonlinear interactions among variables and meaningful shifts in metastatic risk. Age also appeared as a protective factor, with reduced metastatic risk beyond approximately 70 years, aligning with findings in elderly patients (≥ 80 years) [36]. Together, these results reinforce the biological plausibility and clinical relevance of the LiMPC model.

Subgroup analyses revealed performance heterogeneity. The model performed better in older patients (AUROC 0.82 for ≥ 60 vs 0.67 for < 60) and in males (AUROC 0.82 vs 0.76 in females). These findings suggest that the relative contribution of risk factors to liver metastasis differs according to age and sex, rather than being uniform across populations. Therefore, liver metastasis in pancreatic cancer may arise through partially distinct risk pathways depending on demographic background, underscoring the need for tailored risk stratification in clinical practice. Supplementary analyses further demonstrated that predictors of future metastasis were

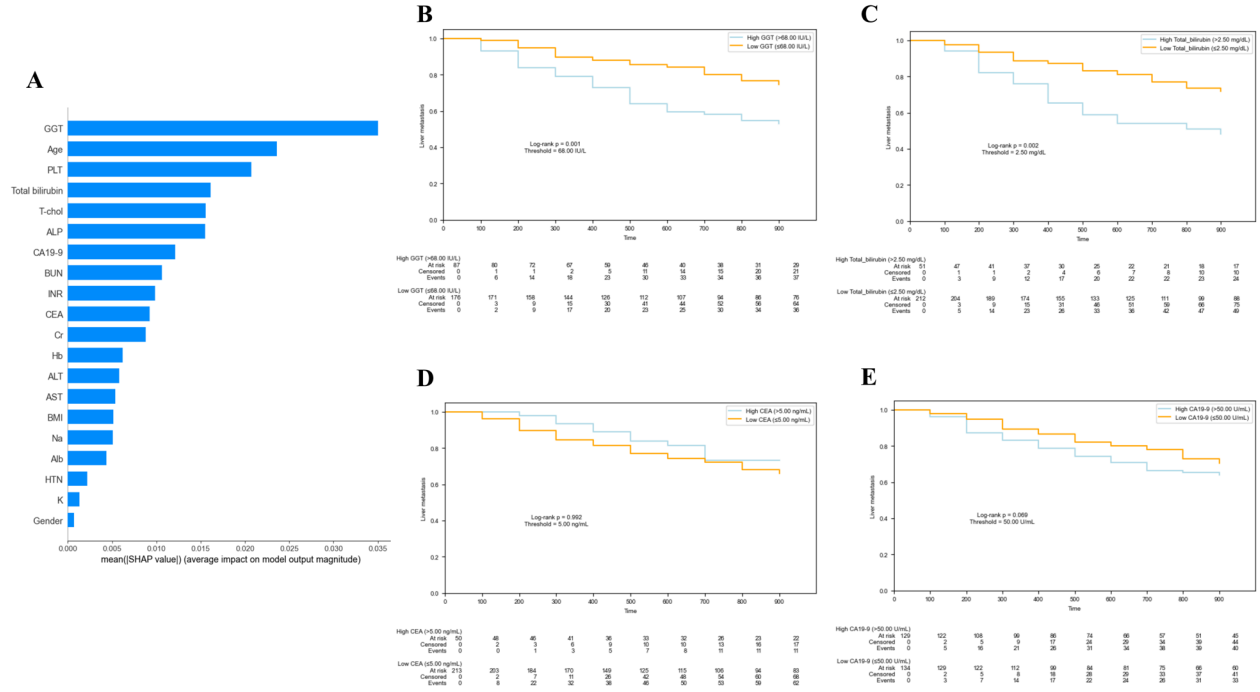

Fig. 6 SHAP analysis and Kaplan–Meier curves for key clinical predictors in the surgical group. **A** SHapley Additive exPlanations (SHAP) analysis using the random survival forest model was conducted in the surgical group. Gamma-glutamyl transferase (GGT), age, platelet count, and total bilirubin were identified as the top predictors. Based on these results and clinical relevance, GGT, total bilirubin, carcinoembryonic antigen (CEA), and carbohydrate antigen 19–9 (CA 19–9) were selected for further survival analysis. For each feature, a log-rank test was performed to stratify patients into two groups using the optimal threshold, which minimized the log-rank *P* value while ensuring that each group included at least 50 patients. **B** Kaplan–Meier survival curves stratified by GGT using a threshold of 68.0 IU/L ($P=0.001$). **C** Kaplan–Meier curve stratified by total bilirubin using a threshold of 2.5 mg/dL ($P=0.002$). **D** Kaplan–Meier curve stratified by CEA using a threshold of 5.0 ng/mL ($P=0.992$). **E** Kaplan–Meier curve stratified by CA 19–9 using a threshold of 50.0 U/mL ($P=0.069$)

generally consistent with baseline predictors; however, in the surgical subgroup, liver function markers such as GGT and total bilirubin were more predictive than tumor markers. This observation supports emerging evidence that the liver microenvironment (including fibrosis or steatosis) plays a role in metastatic seeding [37]. Similar associations have been reported in colorectal, breast, and melanoma cancers [38, 39].

Strengths and future implementation

The strengths of this study include its large cohort, external validation, and use of an interpretable model built entirely from routine clinical data, highlighting timeliness and cost-effectiveness. Clinically, LiMPC may be particularly useful for patients with inconclusive imaging, where predictions above the optimal threshold (≥0.146) could guide deferral of surgery in favour of additional imaging or closer follow-up. By stratifying patients into low- and high-risk groups, LiMPC demonstrates the potential to provide practical decision support beyond simple risk estimation.

This exploratory study shows that simple, routinely available clinical variables can effectively stratify patients and identify subgroups at different metastatic risk. As a readily implementable framework, LiMPC may serve as a foundation for future integration with multi-omics data or emerging biomarkers to advance personalised medicine [40]. Notably, the key predictors identified in this study— such as CA 19-9, CEA— together with demographic differences including sex and age, and risk factors identified from ML-based survival analyses in the initially non-metastatic and surgically treated groups, could inform future research on patient stratification, additional molecular testing, and clinical trial enrolment. These findings highlight LiMPC's potential to bridge diagnostic prediction with precision medicine-oriented trial design [41]. In line with recent integrative and multidisciplinary strategies emphasized by Chen Z et al., LiMPC illustrates how accessible clinical data can be translated into a practical predictive framework that bridges real-world practice with translational innovation [42].

Limitations

Despite its strengths, this study has some limitations. First, as this was a retrospective analysis of an existing pancreatic cancer cohort, the possibility of selection bias cannot be excluded. Therefore, we used a five-fold

cross-validation and external validation to enhance the robustness. Second, Lewis antigen, ctDNA, and imaging features were not included, as we aimed to develop a broadly applicable model using only routine parameters to emphasize simplicity and generalizability. Additional data are being collected to assess their impact. Third, liver metastasis was defined by CT or MRI, which have limited sensitivity for small lesions. To reduce potential misclassification, we included cases detected within 30 days of diagnosis, reflecting real-world practice; however, the possibility of new metastases cannot be fully excluded. Nevertheless, the model maintained stable performance across validation cohorts, suggesting a degree of robustness to label noise. Finally, the model was specialised for liver metastasis in pancreatic cancer and did not account for non-hepatic metastasis. Future work will aim to extend the framework to other metastatic sites to enhance clinical utility.

Conclusion

Overall, LiMPC addresses an unmet need for an interpretable and cost-effective approach to predicting liver metastasis in pancreatic cancer. It enables early risk stratification using only routinely collected clinical data, demonstrating potential to reduce diagnostic delays and support treatment planning. In particular, it may help identify patients at higher risk who could benefit from additional evaluation or closer surveillance in conjunction with imaging findings. LiMPC functions as an exploratory framework showcasing the transformation of routinely collected clinical data into a decision-support tool that may enhance personalized risk stratification and therapeutic planning in oncology.

Abbreviations

ALP	Alkaline phosphatase
ALT	Alanine aminotransferase
AST	Aspartate aminotransferase
AUROC	Area under the receiver operating characteristic
CEA	Carcinoembryonic antigen
CPH	Cox proportional hazards
CT	Computed tomography
DT	Decision tree
DCA	Decision curve analysis
EMR	Electronic medical records
GBSA	Gradient boosting survival analysis
GGT	Gamma-glutamyl transferase
INR	International normalized ratio
LightGBM	Light Gradient Boost Machine
LiMPC	Liver Metastasis in Pancreatic Cancer
ML	Machine learning
MRI	Magnetic resonance imaging
NPV	Negative predictive value
PPV	Positive predictive value
RF	Random forest
RSF	Random survival forest
SHAP	SHapley Additive exPlanations

Supplementary Information

The online version contains supplementary material available at https://doi.org/10.1186/s12885-025-15285-4.

Additional file 1: Supplementary tables S1-S4.

Additional file 2: TRIPOD checklist.

Additional file 3: Supplementary figure S1.

Additional file 4: Supplementary figure S2.

Acknowledgements

We thank the medical record and data management team at all participating hospitals— Ewha Womans University Seoul Hospital, Konkuk University Medical Center, Keimyung University Dongsan Hospital, Gangnam Severance Hospital, and Yongin Severance Hospital—for their assistance with data collection.

Authors' contributions

YGK led data curation and machine learning model development. YGK and HSL wrote the manuscript and designed all figures and tables with input from all coauthors. SYL, WKL, JHP, SHL, KIS, JK, JHK, JHJ, SIJ, JHC, GL, MJC, JYP, SB, SWP, SUK were responsible for validation. HSL, JHJ, and JHC contributed to funding the acquisition. All authors contributed to critical analyses and review of the manuscript.

Funding

We received support from Yonsei University (Seoul, Korea) and National Research Foundation of Korea (NRF) grants funded by the Korean government (MSIT) (RS-2024-00342475, RS-2024-00335625, RS-2023-00222737, and NRF- 2022R1A2C1009842), grant of the Korea Health Technology R&D Project through the Korea Health Industry Development Institute (KHIDI), funded by the Ministry of Health& Welfare, Republic of Korea (grant number : RS-2025-25458830, and RS-2025-25459146).

Data availability

The data generated in this study are not publicly available due to patient privacy restrictions and institutional review board agreement, but are available from the corresponding author on reasonable request.

Declarations

Ethics approval and consent to participate

This study protocol conforms to the ethical guidelines of the 1975 Declaration of Helsinki, as reflected in the prior approval by the institutional review board (IRB) of Severance Hospital (Approval number: 2024–2552-002). The requirement for informed consent was waived by the IRB due to the retrospective nature of the study.

Consent for publication

Not applicable.

Competing interests

The authors declare no competing interests.

Author details

[1]Division of Gastroenterology, Department of Internal Medicine, Severance Hospital, Yonsei University College of Medicine, Seoul, Korea
[2]Institute of Gastroenterology, Yonsei University College of Medicine, Seoul, Korea
[3]Division of Gastroenterology, Department of Internal Medicine, Gangnam Severance Hospital, Yonsei University College of Medicine, Seoul, Korea
[4]Division of Gastroenterology, Department of Internal Medicine, Yongin Severance Hospital, Yonsei University College of Medicine, Seoul, Korea
[5]Division of Gastroenterology, Department of Internal Medicine, Konkuk University School of Medicine, Seoul, Korea
[6]Division of Gastroenterology, Department of Internal Medicine, Keimyung University School of Medicine, Daegu, Korea

[7]Division of Gastroenterology, Department of Internal Medicine, Ewha Womans University College of Medicine, Seoul, Korea
[8]Department of Internal Medicine, Yonsei University College of Medicine, Seoul, Korea
[9]Yonsei Liver Center, Severance Hospital, Seoul, Republic of Korea

Received: 12 August 2025 / Accepted: 31 October 2025
Published online: 27 November 2025

References

1. Li T, Lin C, Wang W. Global, regional, and national burden of pancreatic cancer from 1990 to 2021, its attributable risk factors, and projections to 2050: a systematic analysis of the global burden of disease study 2021. BMC Cancer. 2025;25(1):189.
2. Yokoyama S, Hamada T, Higashi M, Matsuo K, Maemura K, Kurahara H, et al. Predicted prognosis of patients with pancreatic cancer by machine learning. Clin Cancer Res. 2020;26(10):2411–21.
3. Ryan DP, Hong TS, Bardeesy N. Pancreatic adenocarcinoma. N Engl J Med. 2014;371(11):1039–49.
4. Takesue S, Shinkawa T, Otsubo Y, Matsumoto S, Sagara A, Yonenaga A, et al. Neutrophil extracellular traps promote liver micrometastasis in pancreatic ductal adenocarcinoma via the activation of cancer-associated fibroblasts. Int J Oncol. 2020;56(2):596.
5. Kim JH, Hong SS, Kim SH, Hwang HK, Kang CM. Is there a potential oncologic role for local therapy on hepatic metastasis in patients who undergo curative pancreatectomy for pancreatic cancer? Yonsei Med J. 2025;66(6):329–36.
6. Zhou W, Wang D, Lou W. Current role of surgery in pancreatic cancer with synchronous liver metastasis. Cancer Control. 2020;27(1):1073274820976593.
7. Elnahal SM, Shinagare AB, Szymonifka J, Hong TS, Enzinger PC, Mamon HJ. Prevalence and significance of subcentimeter hepatic lesions in patients with localized pancreatic adenocarcinoma. Pract Radiat Oncol. 2012;2(4):e89-94.
8. Gemenetzis G, Groot VP, Blair AB, Ding D, Thakker SS, Fishman EK, et al. Incidence and risk factors for abdominal occult metastatic disease in patients with pancreatic adenocarcinoma. J Surg Oncol. 2018;118(8):1277–84.
9. White R, Winston C, Gonen M, D'Angelica M, Jarnagin W, Fong Y, et al. Current utility of staging laparoscopy for pancreatic and peripancreatic neoplasms. J Am Coll Surg. 2008;206(3):445–50.
10. Litjens G, Rivière DM, van Geenen EJM, Radema SA, Brosens LAA, Prokop M, et al. Diagnostic accuracy of contrast-enhanced diffusion-weighted MRI for liver metastases of pancreatic cancer: towards adequate staging and follow-up of pancreatic cancer - DIA-PANC study: study protocol for an international, multicenter, diagnostic trial. BMC Cancer. 2020;20(1):744.
11. Kim HJ, Lee SS, Byun JH, Kim JC, Yu CS, Park SH, et al. Incremental value of liver MR imaging in patients with potentially curable colorectal hepatic metastasis detected at CT: a prospective comparison of diffusion-weighted imaging, gadoxetic acid-enhanced MR imaging, and a combination of both MR techniques. Radiology. 2015;274(3):712–22.
12. Riviere DM, van Geenen EJM, van der Kolk BM, Nagtegaal ID, Radema SA, van Laarhoven CJHM, et al. Improving preoperative detection of synchronous liver metastases in pancreatic cancer with combined contrast-enhanced and diffusion-weighted MRI. Abdom Radiol. 2019;44(5):1756–65.
13. Azari FS, Vollmer CM Jr, Roses RE, Keele L, DeMatteo RP, Drebin JA, et al. A contemporary analysis of palliative procedures in aborted pancreatoduodenectomy: morbidity, mortality, and impact on future therapy. Surgery. 2020;168(6):1026–31.
14. Sonkin D, Thomas A, Teicher BA. Cancer treatments: Past, present, and future. Cancer Genet. 2024;286–287:18–24.
15. Meisel JL, Venur VA, Gnant M, Carey L. Evolution of targeted therapy in breast cancer: where precision medicine began. Am Soc Clin Oncol Educ Book. 2018;38:78–86.
16. Schechter AL, Stern DF, Vaidyanathan L, Decker SJ, Drebin JA, Greene MI, et al. The *neu* oncogene: an *erb*-B-related gene encoding a 185,000-Mr tumour antigen. Nature. 1984;312:513–6.
17. Crosby D, Bhatia SN, Brindle KM, Coussens LM, Dive C, Emberton M, et al. Early detection of cancer. Science. 2022;375(6586):eaay9040. https://doi.org/10.1126/science.aay9040.
18. Poruk KE, Gay DZ, Brown K, Mulvihill JD, Boucher KM, Scaife CL, et al. The clinical utility of CA 19–9 in pancreatic adenocarcinoma: diagnostic and prognostic updates. Curr Mol Med. 2013;13(3):340–51.
19. National Comprehensive Cancer Network. Pancreatic Adenocarcinoma (Version 3.2024). Available from: https://www.nccn.org/guidelines/guidelines-detail?category=1&id=1455.
20. Jiang G, Zhou X, Chen S, Zhong F, Huang G, Wu B, et al. SATB2 plays a critical role in pancreatic cancer cell proliferation, migration and T cell cytotoxicity. Cancer Genet. 2025;296–297:53–64.
21. Ren S, Song LN, Zhao R, Tian Y, Wang ZQ. Serum exosomal hsa-let-7f-5p: a potential diagnostic biomarker for metastatic pancreatic cancer detection. World J Gastroenterol. 2025;31(26):109500.
22. Moons KG, Altman DG, Reitsma JB, Ioannidis JP, Macaskill P, Steyerberg EW, et al. Transparent Reporting of a multivariable prediction model for Individual Prognosis or Diagnosis (TRIPOD): explanation and elaboration. Ann Intern Med. 2015;162(1):W1-73.
23. Murorunkwere BF, Ihirwe JF, Kayijuka I, Nzabanita J, Haughton D. Comparison of tree-based machine learning algorithms to predict reporting behavior of electronic billing machines. Information. 2023;14(3):140.
24. Vickers AJ, Van Calster B, Steyerberg EW. Net benefit approaches to the evaluation of prediction models, molecular markers, and diagnostic tests. BMJ. 2016;352:i6.
25. Wang H, Liang Q, Hancock JT, Khoshgoftaar TM. Feature selection strategies: a comparative analysis of SHAP-value and importance-based methods. J Big Data. 2024;11(1):44.
26. Yuan C, Kim J, Wang QL, Lee AA, Babic A, Amundadottir LT, et al. The age-dependent association of risk factors with pancreatic cancer. Ann Oncol. 2022;33(7):693–701.
27. Bojmar L, Zambirinis CP, Hernandez JM, Chakraborty J, Shaashua L, Kim J, et al. Multi-parametric atlas of the pre-metastatic liver for prediction of metastatic outcome in early-stage pancreatic cancer. Nat Med. 2024;30(8):2170–80.
28. Mehdorn AS, Gemoll T, Busch H, Kern K, Beckinger S, Daunke T, et al. Biomarkers in liquid biopsies for prediction of early liver metastases in pancreatic cancer. Cancers (Basel). 2022;14(19):4605. https://doi.org/10.3390/cancers14194605.
29. Heredia-Soto V, Rodríguez-Salas N, Feliu J. Liquid biopsy in pancreatic cancer: are we ready to apply it in the clinical practice? Cancers (Basel). 2021;13(8):1986. https://doi.org/10.3390/cancers13081986.
30. Imaoka H, Mizuno N, Hara K, Hijioka S, Tajika M, Tanaka T, et al. Prognostic impact of carcinoembryonic antigen (CEA) on patients with metastatic pancreatic cancer: a retrospective cohort study. Pancreatology. 2016;16(5):859–64.
31. Lee KJ, Yi SW, Chung MJ, Park SW, Song SY, Chung JB, et al. Serum CA 19–9 and CEA levels as a prognostic factor in pancreatic adenocarcinoma. Yonsei Med J. 2013;54(3):643.
32. Kim TH, Han S-S, Park S-J, Lee WJ, Woo SM, Yoo T, et al. CA 19–9 level as indicator of early distant metastasis and therapeutic selection in resected pancreatic cancer. Int J Radiat Oncol Biol Phys. 2011;81(5):e743–8.
33. Raza SS, Khan H, Hajibandeh S, Hajibandeh S, Bartlett D, Chatzizacharias N, et al. Can preoperative carbohydrate antigen 19–9 predict metastatic pancreatic cancer? Results of a systematic review and meta-analysis. HPB (Oxford). 2024;26(5):630–8.
34. Kim YC, Kim HJ, Park JH, Park DI, Cho YK, Sohn CI, et al. Can preoperative CA19-9 and CEA levels predict the resectability of patients with pancreatic adenocarcinoma? J Gastroenterol Hepatol. 2009;24(12):1869–75.
35. van Manen L, Groen JV, Putter H, Vahrmeijer AL, Swijnenburg RJ, Bonsing BA, et al. Elevated CEA and CA19-9 serum levels independently predict advanced pancreatic cancer at diagnosis. Biomarkers. 2020;25(2):186–93.
36. Huang J, Li X, Jiang Q, Qiu H, Rong Y, Cui B, et al. Analysis of risk factors for distant metastasis of pancreatic ductal adenocarcinoma without regional lymph node metastasis and a nomogram prediction model for survival. Evid Based Complement Alternat Med. 2023;2023:2916974.
37. Tsilimigras DI, Brodt P, Clavien P-A, Muschel RJ, D'Angelica MI, Endo I, et al. Liver metastases. Nat Rev Dis Primers. 2021;7(1):27.
38. Li Y, Su X, Rohatgi N, Zhang Y, Brestoff JR, Shoghi KI, et al. Hepatic lipids promote liver metastasis. JCI Insight. 2020;5(17):e136215. https://doi.org/10.1172/jci.insight.136215.
39. Kondo T, Okabayashi K, Hasegawa H, Tsuruta M, Shigeta K, Kitagawa Y. The impact of hepatic fibrosis on the incidence of liver metastasis from colorectal cancer. Br J Cancer. 2016;115(1):34–9.
40. Joshi RM, Telang B, Soni G, Khalife A. Overview of perspectives on cancer, newer therapies, and future directions. Oncology and Translational Medicine. 2024;10(3):105–9.

41. Noreen M, Devika B, Suso P. Fast-tracking drug development with biomarkers and companion diagnostics. J Cancer Metastasis Treat. 2024;10:3.
42. Chen Z, Saw PE. Integration in biomedical science 2024: emerging trends in the post-pandemic era. BIO Integration. 2024;5(1):e1001.

Publisher's Note